Proteomics Analysis of the Interactome of N-myc Downstream Regulated Gene 1 and Its Interactions with the Androgen Response Program in Prostate Cancer Cells*[S]

Lan Chun Tu, Xiaowei Yan, Leroy Hood, and Biaoyang Lin‡

NDRG1 is known to play important roles in both androgen-induced cell differentiation and inhibition of prostate cancer metastasis. However, the proteins associated with NDRG1 function are not fully enumerated. Using coimmunoprecipitation and mass spectrometry analysis, we identified 58 proteins that interact with NDRG1 in prostate cancer cells. These proteins include nuclear proteins, adhesion molecules, endoplasmic reticulum (ER) chaperons, proteasome subunits, and signaling proteins. Integration of our data with protein-protein interaction data from the Human Proteome Reference Database allowed us to build a comprehensive interactome map of NDRG1. This interactome map consists of several modules such as a nuclear module and a cell membrane module; these modules explain the reported versatile functions of NDRG1. We also determined that serine 330 and threonine 366 of NDRG1 were phosphorylated and demonstrated that the phosphorylation of NDRG1 was prominently mediated by protein kinase A (PKA). Further, we showed that NDRG1 directly binds to β-catenin and E-cadherin. However, the phosphorylation of NDRG1 did not interrupt the binding of NDRG1 to E-cadherin and β-catenin. Finally, we showed that the inhibition of NDRG1 expression by RNA interference decreased the ER inducible chaperon GRP94 expression, directly proving that NDRG1 is involved in the ER stress response. Intriguingly, we observed that many members of the NDRG1 interactome are androgen-regulated and that the NDRG1 interactome links to the androgen response network through common interactions with β-catenin and heat shock protein 90. Therefore we overlaid the transcriptomic expression changes in the NDRG1 interactome in response to androgen treatment and built a dual dynamic picture of the NDRG1 interactome in response to androgen. This interactome map provides the first road map for understanding the functions of NDRG1 in cells and its roles in human diseases, such as prostate cancer, which can progress from androgen-dependent curable stages to androgen-independent incurable stages. ***Molecular & Cellular Proteomics 6:575–588, 2007.***

From the Institute for Systems Biology, Seattle, Washington 98103
Received, July 6, 2006, and in revised form, January 9, 2007
Published, MCP Papers in Press, January 12, 2007, DOI 10.1074/mcp.M600249-MCP200

N-myc downstream regulated gene 1 (NDRG1)[1] is known to be involved in cell differentiation, carcinogenesis, atherosclerosis, survival, and metastasis (1). The induction of NDRG1 expression is associated with the processes of cell differentiation such as trophoblast recovery from hypoxia-induced injury (2) and mast cell maturation (3). Therefore, it has been characterized as a differentiation-regulated gene (4, 5). The expression levels of NDRG1 in normal and cancer tissue remain controversial. Some studies showed that NDRG1 is down-regulated in cancer such as prostate, breast, and colon (6–8). Other studies showed that NDRG1 is overexpressed in a variety of cancers including lung, brain, melanoma, liver, prostate, breast, and renal cancers (9). Nonetheless, overexpression of NDRG1 is known to inhibit tumor growth and metastasis by inducing cell differentiation (10, 11). Thus it is postulated that NDRG1 can be a tumor suppressor and a potential marker for cancer diagnosis (9–11). Wang *et al.* (12) showed that increased expression of NDRG1 was correlated with tumor progression during colorectal carcinogenesis. In contrast, others demonstrated that NDRG1 was induced in primary colon carcinoma but reduced in metastatic colon cancer (11). Overexpression of NDRG1 in highly metastatic colon cancer cells resulted in the suppression of cancer cell invasion and metastasis both *in vitro* and *in vivo* (8). Moreover, NDRG1 expression was significantly reduced in patients with lymph node or bone metastasis as compared with those with localized prostate cancer (6). These evidences indicate that NDRG1 can be a metastasis suppressor and may be a predictor of cancer metastasis (12). However, how NDRG1 mediates its multiple functions remains largely unknown.

NDRG1 belongs to a new family of proteins that contains no protein motifs of known function (13). It is a cytoplasmic protein that contains three 10-amino acid tandem repeats at the C terminus (4) and is also a phosphoprotein that can be phosphorylated by several protein kinases (14). NDRG1 was categorized into the α/β hydrolase superfamily based on protein structure, but it does not have a catalytic site (15). The

[1] The abbreviations used are: NDRG1, N-myc downstream regulated gene 1; ER, endoplasmic reticulum; PKA, protein kinase A; IP, immunoprecipitation; DRB, 5,6-dichloro-1-β-D-ribofuranosylbenzimidazole; PCNA, proliferating cell nuclear antigen; siRNA, short interfering RNA; FBS, fetal bovine serum; PKC, protein kinase C; HPRD, Human Protein Reference Database; MPSS, massively parallel signature sequencing; AR, androgen receptor; Suc-LLVY-AMC, *N*-succinyl-Leu-Leu-Val-Tyr-7-amido-4-methylcoumarin.

expression of NDRG1 can be induced by a variety of stimulus including ER stress-inducing agents such as β-mercaptoethanol and tunicamycin (16). We and others have shown that NDRG1 expression was induced by androgen (17, 18). Phosphatase and tensin homolog (PTEN) (7) and p53 (10), two important tumor suppressor genes, also up-regulate the expression of NDRG1. Other inducers include metal ions (19–22), DNA damage agents such as camptothecin (23), intracellular calcium concentrations (24), and hypoxic condition (25). Hypoxia and its mimetics (*e.g.* nickel and cobalt) are probably the most important inducers of the NDRG1 gene (26). Nickel and cobalt induce NDRG1 expression by creating hypoxia-like conditions in cells (20). Like other hypoxia responsive genes, the induction of NDRG1 is prominently mediated by the transcription factor HIF-1α (20, 27). HIF-1α induces NDRG1 through a phosphatidylinositol 3-kinase/Akt-dependent pathway (28), but HIF-1-independent pathways may also be involved (29). These results imply that multiple proteins and pathways contribute to the regulation of NDRG1.

Although we know a lot about the genomic actions that regulate NDRG1 expression, we know little about the non-genomic regulation of NDRG1 at the protein level, which includes the proteins that interact with NDRG1 (the NDRG1 interactome) and execute its versatile functions in both normal and abnormal physiological conditions. With the advance of mass spectrometry technology, we sought to comprehensively profile the NDRG1 interactome by immunoprecipitation coupled with high throughput tandem mass spectrometric analysis. Because NDRG1 is an androgen-regulated gene, we conducted the experiments in androgen-treated prostate cancer cells LNCaP to gain additional information on the relationship between the androgen response network and the NDRG1 interactome.

We identified 58 novel NDRG1-interacting proteins by immunoprecipitation (IP)-LC/MS/MS and demonstrated that NDRG1 directly binds to β-catenin and E-cadherin. Intriguingly, the NDRG1 interactome links to the androgen network through interactions with β-catenin and heat shock protein 90. The identified NDRG1 interacting proteins also correlate well with the functions of NDRG1 including NDRG1 phosphorylation, the regulation of ER chaperon expression, and proteasome activity.

EXPERIMENTAL PROCEDURES

Materials—Synthetic androgen methyltrienolone (R1881) was purchased from PerkinElmer Life Sciences. R1881 (10 mM) stock solution was prepared in ethanol and stored at −20 °C. Kinase inhibitors including H-89, GF109203X, KN-62, and 5,6-dichloro-1-β-D-ribofuranosylbenzimidazole (DRB) were purchased from Sigma-Aldrich. Stock solutions (10 mM) were prepared in DMSO and stored at −20 °C. Proteasome substrate III Z-LLL AMC was purchased from Calbiochem and was dissolved in DMSO, stored at −20 °C. Protein A-Sepharose was purchased from Invitrogen. IgY microbeads and anti-NDRG1 polyclonal IgY and rabbit anti-IgY antibodies were purchased from GenWay Biotech (San Diego, CA). Monoclonal antibody against E-cadherin and β-catenin was ordered from BD Transduction Laboratories, monoclonal antibody against proliferating cell nuclear antigen (PCNA) was from Millipore Corporation, and antibody against amino acid residue KDEL in the protein GRP78 and TRA1 was from Abcam Inc. (Cambridge, MA). Trypsin and ECL reagent were purchased from Amersham Biosciences. NDRG1 siRNA smart pool and Dharmafect 3 reagent were purchased from Dharmacon (Lafayette, CO).

Cell Culture and Treatments—Human prostate cancer cell line LNCaP was obtained from American Type Culture Collection (ATCC, Rockville, MD) and maintained in phenol red-free RPMI 1640 medium supplemented with 10% fetal bovine serum (FBS), 100 units/ml penicillin, and 100 μg/ml streptomycin at 37 °C under 5% CO_2. For androgen deprivation, LNCaP cells were cultured in phenol red-free RPMI 1640 medium with 10% dextran-coated charcoal-stripped FBS for 60 h prior to treatment with 10 nM R1881 or siRNA transfection. All treatments were done in phenol red-free RPMI 1640 medium with 10% dextran-coated charcoal-stripped FBS. For treatment of cells with protein kinase inhibitors, cells were pretreated for 30 min with 10 μM H-89 (protein kinase A inhibitor), 2 μM GF109203X (protein kinase C (PKC) inhibitor), 10 μM KN-62 (calcium-calmodulin kinase II inhibitor) (Sigma), 10 μM DRB (casein kinase-II inhibitor), or vehicle control (DMSO) in medium.

Immunoblotting—Cells were washed twice with PBS and lysed at 4 °C in a lysis buffer (50 mM Hepes, pH 7.4, 4 mM EDTA, 2 mM EGTA, 10 mM sodium fluoride, 2 mM sodium pyrophosphate, 1% Triton X-100, 2 μM PMSF, 1× protease inhibitor mixture, 1 mM Na_3VO_4). Lysates were centrifuged at 14,000 rpm for 20 min. The protein concentration in the lysates was determined using the Bio-Rad protein assay kit. Cell lysates were subjected to SDS-PAGE electrophoresis and transferred to a PVDF membrane (Hybond-P, Amersham Biosciences). The membrane was blocked with 4% nonfat milk in TBS (25 mM Tris, pH 7.4, 125 mM NaCl) for 1 h at room temperature followed by incubation with primary antibodies against NDRG, PCNA, and KDEL. The membranes were washed 3 times with TBS and then incubated with horseradish peroxidase conjugated anti-rabbit IgY or anti-mouse IgG for 1 h. The immunoblot was then washed five times with TBS and developed using ECL. Experiments were repeated at least three times.

Coimmunoprecipitation—Cell lysates were incubated with 10 μl of IgY microbeads or 30 μl of protein A-Sepharose for 1 h at 4 °C to eliminate nonspecific absorption of proteins to the beads. After brief centrifugation, the supernatants were incubated for 1 h at 4 °C with IgY-microbeads or protein A-Sepharose that had been incubated with anti-NDRG1, anti-E-cadherin, anti-β-catenin, anti-Ku70, or anti-CANX antibodies overnight at 4 °C. Beads were then washed twice with buffer B (20 mM Tris-HCl, pH 7.4, 0.5 M NaCl) and twice with buffer C (20 mM Tris-HCl, pH 7.4, 0.5 mM DTT). After washing, the beads were boiled with SDS sample buffer and analyzed by SDS-PAGE. After SDS-PAGE electrophoresis, proteins were transferred to PVDF membrane and followed by Western blotting with anti-NDRG1, anti-E-cadherin, anti-β-catenin, anti-Ku70, or anti-CANX antibodies. For MS analysis, proteins were detected by silver staining and followed by in-gel trypsin digestion.

In-gel Trypsin Digestion—For mass spectrometry analysis, the gels were silver stained. Proteins of interest were cut from gels. Each excised gel was placed in an Eppendorf tube, cut into smaller (less than 1 mm in each dimension) pieces, and incubated with 100 mM ammonium bicarbonate for 1 h. The solution was discarded. The gel pieces were then incubated in 100 mM ammonium bicarbonate containing 45 mM DTT at 60 °C for 30 min. After cooling to room temperature, the DTT solution was replaced with 100 mM iodoacetamide in 100 mM ammonium bicarbonate for 30 min at room temperature in the dark. The gel pieces were washed in 50% acetonitrile, 100 mM ammonium bicarbonate for 1 h, dehydrated in 100% acetonitrile, and dried. The gel pieces were swollen in a digestion buffer containing 25 mM ammonium bicarbonate and 250 ng of trypsin. Following enzymatic digestion overnight at 37 °C, the peptides were extracted with 50 μl of 5% acetonitrile for 15 min at 37 °C followed by addition of 100

μl of 100% acetonitrile for another 15 min at 37 °C. The peptides were then dried and rehydrated in 1% formic acid.

Mass Spectrometry Analysis—Proteins were visualized on SDS-PAGE by silver stain. Bands of interest were excised and subjected to trypsin digestion. Peptides were analyzed by microcapillary high pressure liquid chromatography nanoelectrospray tandem mass spectrometry on a LTQ mass spectrometer (Thermo Electron).

The sample was loaded automatically onto a 2-cm-long 5 μm 200A Magic C18 (Michrom Bioresources) precolumn using a FAMOS autosampler (Dionex). The sample was washed for 15 min with a solution of 5% acetonitrile, 0.1% formic acid. A gradient was then delivered from 10 to 35% acetonitrile over 30 min. This eluted the peptides off of the precolumn onto a 10-cm-long 5 μm 100A Magic C18 analytical column and then finally into the LTQ. Both the wash and the gradient were delivered using an Aglient 1100 series binary pump, and the gradient was followed by a cleaning and equilibration step. Thermo LTQ mass spectrometer parameters were as follows: Ion Max™ source with sweep cone, ESI probe, capillary temperature 250 °C, sheath gas flow 0, auxiliary gas flow 0, Sweep gas flow 0, positive polarity: source voltage 2 kV, capillary voltage 16 V, tube lens (V) 55.00.

LC/MS spectra were acquired using 4 scans events. Data-dependent acquisition was set to require a minimal signal of 1000. We used the SEQUEST database to match peptide tandem mass spectra to sequences in the human International Protein Index (IPI) database (3.17) (30). The SEQUEST parameter file is shown in supplemental Doc 1. We used the Peptide Prophet and Protein Prophet programs to measure the quality of peptide and protein identification (31, 32). To assess the MS spectra quality, we applied a filter with a Protein Prophet probability >0.9 (31) and then performed visual inspection of the spectra.

siRNA Transfection—Dharmafect was used for transfection of siRNAs into LNCaP cells according to protocols provided by Dharmacon. Expression of NDRG1 was monitored by Western blotting.

Proteasome Function Assays—Proteasome function was measured as described previously (33), with some minor modifications. To measure 26S proteasome activity, 100-μg proteins of cell lysates were diluted with buffer I (50 mM Tris (pH 7.4), 2 mM DTT, 5 mM $MgCl_2$, 2 mM ATP) to a final volume of 200 μl in triplicate. The fluorogenic proteasome substrate Suc-LLVY-AMC (chymotrypsin-like, Calbiochem) was dissolved in DMSO and added to a final concentration of 80 μM in 1% DMSO. Proteolytic activity was measured as the release of the fluorescent group 7-amido-4-methylcoumarin in a fluorescence plate reader (BioTex FLx800™, Winooski, VT) at 380/460 nm.

RESULTS

Interactome of NDRG1: NDRG1-interacting Proteins Identified by Immunoprecipitation and LC/MS/MS—To explore proteins that interact with NDRG1, we performed a proteomics analysis of the NDRG1 containing complex by IP coupled with LC/MS/MS. Because androgen dramatically increases NDRG1 protein expression (see Fig. 2*A*), we used LNCaP cells treated with 10 nM R1881 for 24 h for the IP experiment. The IP complex was eluted, separated on SDS-PAGE, and subjected to in-gel trypsin digestion. The tryptic digests were analyzed through microcapillary liquid chromatography MS/MS followed by protein database searching of the acquired spectra. To control for nonspecific IP, IgY preimmune complex was also analyzed. The experiments were performed in three replicates, and each replicate was run through MS/MS three times. Fifty-eight proteins were identified in the NDRG1 complex after 1) filtering proteins that had a Protein Prophet probability >0.9 (31) and passed visual inspection to assess the MS spectra quality, 2) removing proteins that were not found in the replicate experiments, and 3) subtracting common proteins that were found in the IgY preimmune complex. One known NDRG1 interacting partner heat shock protein 70 (34) was excluded from the list because it was also identified from the IgY control IP/MS analysis.

The identified proteins can be classified into several functional categories such as ER chaperons, vesicle-mediated protein trafficking, DNA repair and transcription, cell adhesion and cytoskeleton organization, signal transduction, RNA processing, protein translation, and metabolism (Table I). Most of the proteins identified in the NDRG1 complex correlate well with the reported functions of NDRG1 such as differentiation, metastasis, and ER stress responses. All the protein interactions identified here were novel.

Since this study was performed under androgen-stimulated conditions, many proteins that were identified from the NDRG1 complex are also known androgen-regulated proteins such as heat shock protein 90 α (HSPCA), β-catenin (CTNNB1), calnexin (CANX), SEC23, 26S protease regulatory subunit 7 (PSMC2), and 26S protease regulatory subunit 6A (PSMC3). Based on the identified NDRG1-interacting proteins, we retrieved protein-protein interactions from the Human Protein Reference Database (HPRD, www.hprd.org) and built a map of the interactome of NDRG1 (Fig. 1). Interestingly, the NDRG1 interactome can link to the androgen receptor interactome (www.hprd.org) through CTNNB1 and HSPCA.

To understand the androgen regulation of the proteins in the NDRG1 interactome map, the androgen-responsive expression levels of each gene were also indicated on the map (*colored circles*, Fig. 1). Expression levels were measured using massively parallel signature sequencing (MPSS) analysis (35, 36) comparing of LNCaP cells that had been treated with R1881 against untreated cells.[2] Only those genes with a Z-test p value < 0.05 were indicated, and the *red-colored* nodes indicate androgen up-regulated (p value < 0.05) genes, and *green-colored* nodes indicate androgen down-regulated ($p < 0.05$) genes.

Confirmation of the Interactome of NDRG1: E-cadherin and β-Catenin Interact with NDRG1—Our proteomics analysis revealed many interesting protein interactions for NDRG1. To confirm our IP-LC/MS/MS analysis results, we selected two interesting protein candidates and confirmed their binding to NDRG1 by reciprocal coimmunoprecipitation and Western blot based on the availability and quality of the available antibodies.

First we chose β-catenin and its binding partner E-cadherin. Interestingly, E-cadherin was also identified in the NDRG1 IP complex. However, it was only identified in two of three replicate experiments and therefore not included in Ta-

[2] X. Yan, L. Hood, and B. Lin, unpublished results.

TABLE I
Proteins identified from NDRG1 IP complex by LC-MS/MS analysis

Gene symbol	Total no. of peptides	No. of independent experiments	IPI	RefSeq accession no.	Protein description	Amino acid coverage
						%
NDRG1	23	3	IPI00022078	NP_006087	NDRG1	28.2
Chaperon protein						
HSPCA	57	3	IPI00382470	NP_005339	Heat shock protein HSP 90-α	44.7
HSPA5 (GRP78)	79	3	IPI00003362	NP_005338	Heat shock 70 kDa protein 5	42
VCP	19	3	IPI00022774	NP_009057	Transitional endoplasmic reticulum ATPase	23.2
CANX	18	3	IPI00020984	NP_001737	Calnexin	21.5
Ubiquitin-dependent protein catabolism	22	3	IPI00018398	NP_002795	26S protease regulatory subunit 6A	32.1
PSMC2	17	3	IPI00021435	NP_002794	26S protease regulatory subunit 7	25.5
PSMD2	32	3	IPI00012268	NP_002799	26S proteasome non-ATPase regulatory subunit 2	37.1
DNA repair proteins						
XRCC6 (Ku70)	32	3	IPI00465430	NP_001460	ATP-dependent DNA helicase II	48.8
RUVBL2	8	3	IPI00009104	NP_006657	RuvB-like 2	21.9
Transcriptional factor						
ILF3 (NFAT90)	16	3	IPI00219330	NP_036350	Interleukin enhancer-binding factor 3	19.5
SEC23A	19	3	IPI00017375	NP_006355	Protein transport protein Sec23A	23
COPB2	54	3	IPI00220219	NP_004757	Coatomer β subunit	36.7
CLTC	86	3	IPI00024067	NP_004850	Similar to clathrin heavy chain	27.2
AP2M1	5	3	IPI00022256	NP_004059	AP-2 complex subunit μ-1	12.5
AP1M2	28	3	IPI00002552	NP_005489	Splice isoform 1 of AP-1 complex subunit μ-2	31
Cell adhesion and cytoskeleton organization	38	3	IPI00247063	NP_009218	Neprilysin	40.9
CTNNB1	39	3	IPI00017292	NP_001895	Splice isoform 1 of β-catenin	38.7
ACTB	50	3	IPI00021440	NP_001605	Actin	60.5
KIF5B	12	3	IPI00012837	NP_004512	Kinesin heavy chain	13.6
Signal transduction						
PPP2R2A	17	3	IPI00332511	NP_002708	Serine/threonine protein phosphatase 2A	31.3
TLE3	3	3	IPI00219368	NP_005069	Splice isoform 1 of transducin-like enhancer protein 3	3.4
Metabolic enzymes, mitochondria precursors, and carrier	11	3	IPI00019912	NP_000405	Peroxisomal multifunctional enzyme type 2	16.5
HSD17B4						
CNDP2	31	3	IPI00177728	NP_060705	Cytosolic nonspecific dipeptidase	33.5
DARS	38	3	IPI00216951	NP_001340	Aspartyl-tRNA synthetase	48.1
DLST	14	3	IPI00420108	NP_001924	Dihydrolipoyllysine-residue succinyl-transferase	13.9
ACSL3	16	3	IPI00401055	NP_004448	acyl-CoA synthetase long chain family member 3	16.7
FASN	33	3	IPI00645907	NP_004095	Fatty acid synthase	11.5
MAOA	26	3	IPI00008483	NP_000231	Amine oxidase (flavin containing) A	25.2
LDHA	14	3	IPI00217966	NP_005557	Lactate dehydrogenase A	22.6
PKM2	41	3	IPI00479186	NP_002645	Pyruvate kinase 3 isoform 1	40.9
RPN2	18	3	IPI00301271	NP_002942	Dolichyl-diphosphooligosaccharide—protein glycosyltransferase 63 kDa subunit precursor	31.9
TARS	29	3	IPI00329633	NP_689508	Threonyl-tRNA synthetase, cytoplasmic	23.7
SHMT2	11	3	IPI00002520	NP_005403	Serine hydroxymethyltransferase, mitochondrial precursor	19.8
SLC25A6	3	3	IPI00291467	NP_001627	Solute carrier family 25,ADP/ATP translocase 3	16.8
ATP1A1	23	3	IPI00006482	NP_000692	Sodium/potassium-transporting ATPase α-1	17.4
Protein translation regulators EEF2	37	3	IPI00186290	NP_001952	Elongation factor 2	28.7
EEF1G	38	3	IPI00000875	NP_001395	Similar to elongation factor 1-gamma	37.2
EIF2S3	15	3	IPI00297982	NP_001406	Eukaryotic translation initiation factor 2 subunit 3	33.1

TABLE I—*continued*

Gene symbol	Total no. of peptides	No. of independent experiments	IPI	RefSeq accession no.	Protein description	Amino acid coverage
						%
EIF3S6	11	3	IPI00013068	NP_001559	Eukaryotic translation initiation factor 3 subunit 6	24.7
PABPC1	52	3	IPI00008524	NP_002559	Splice isoform 1 of polyadenylate-binding protein 1	42.9
Ribosomal proteins						
RPS3	35	3	IPI00011253	NP_000996	40S ribosomal protein S3	57.2
RPS6	17	3	IPI00021840	NP_001001	40S ribosomal protein S6	21.3
RPL24	7	3	IPI00306332	NP_000977	60S ribosomal protein L24	13.4
RPL3	31	3	IPI00550021	NP_000958	60S ribosomal protein L3	34.3
RPS16	15	3	IPI00221092	NP_001011	40S ribosomal protein S16	24.8
RPS8	13	3	IPI00216587	NP_001003	40S ribosomal protein S8	31.9
RPS20	6	3	IPI00012493	NP_001014	40S ribosomal protein S20	25.2
RPS9	18	3	IPI00221088	NP_001004	40S ribosomal protein S9	30.6
RPL4	79	3	IPI00003918	NP_000959	60S ribosomal protein L4	39.2
RPS26	9	3	IPI00655650	NP_001020	40S ribosomal protein S26	21.1
RNA processing						
NCL	21	3	IPI00444262	NP_005372	Nucleolin	25.2
HNRPF	25	3	IPI00003881	NP_004957	Heterogeneous nuclear ribonucleoprotein F	20.5
HNRPU	22	3	IPI00644079	NP_114032	Heterogeneous nuclear ribonucleoprotein U	18.5
HNRPH1	25	3	IPI00013881	NP_005511	Heterogeneous nuclear ribonucleoprotein H1	20.5
DDX1	22	3	IPI00293655	NP_004930	ATP-dependent helicase DDX1	29.5
DDX5	6	3	IPI00017617	NP_004387	Probable RNA-dependent helicase p68	17.6
UPF1	21	3	IPI00034049	NP_002902	Regulator of nonsense transcripts 1	19.2
EWSR1	11	3	IPI00009841	NP_005234	EWS-B of RNA-binding protein EWS	15.5

ble I. LNCaP cells were treated with or without 10 nM R1881 for 24 h, and then cell lysates were immunoprecipitated with anti-NDRG1 IgY antibody. The immune complex was then separated using SDS-PAGE and subjected to Western blot analysis using anti-NDRG1 IgY, anti-E-cadherin, or anti-β-catenin antibodies. To avoid the interference of IgY heavy chain that co-migrate with NDRG1, the IP complex was processed without DTT for the detection of NDRG1.

As shown in Fig. 2*B*, β-catenin was detected in the NDRG1 IP complex but not in the IgY preimmune control. Since R1881 induced high levels expression of NDRG1, the levels of NDRG1 in the untreated cells were too low to be detected within the short (1 s) exposure. Longer exposure revealed that there was basal NDRG1 expression in the androgen-starved (not R1881-treated) cells and that the basal expression is sufficient for the IP. Interestingly, although NDRG1 is dramatically increased after R1881 treatment, the levels of E-cadherin and β-catenin in the NDRG1-IP complex did not increase after exposure to R1881.

Cell lysates were also immunoprecipitated with E-cadherin (Fig. 2*C*) or β-catenin (Fig. 2*D*) antibodies followed by Western blot analysis with anti-NDRG1 IgY antibody. As shown in Fig. 2, *C* and *D*, NDRG1 was detected in both E-cadherin and β-catenin IP complexes. Although weak ladders resulted from protein A appearing at the same position as NDRG1 in the IgG preimmune control, the NDRG1 signal is generally stronger in both E-cadherin and β-catenin IP complexes (Fig. 2, *C* and *D*, *bottom panels*). However, compared with the untreated control cells, the amount of NDRG1 pulled down by E-cadherin and β-catenin was not changed by R1881 stimulation.

Although β-catenin was reduced after R1881 treatment (Fig. 2*D*), the level of NDRG1 and E-cadherin in the β-catenin immune complex was similar to that in the untreated control, indicating that there may be unbound β-catenin present in the untreated cells or that it may bind to other proteins. Consistent with other studies (37), E-cadherin was detected in β-catenin IP complexes, and β-catenin was detected in E-cadherin IP complexes. We showed that NDRG1 was detected in both E-cadherin and β-catenin IP complexes, suggesting that these three proteins form a complex. The binding of NDRG1 to E-cadherin and β-catenin was also confirmed by an *in vitro* binding assay in which GST-NDRG1 was used as a bait to pull down E-cadherin and β-catenin from R1881-treated cell lysates (data not shown).

To confirm additional NDRG1 interacting proteins by the same approach, we purchased ~16 antibodies that were available on the market against the proteins in Table I. Unfortunately, most of them did not work adequately in the IP experiment. Ku70 (XRCC6) and CANX antibodies are two antibodies that performed adequately in the IP experiment. Both Ku70 and CANX were detected in the NDRG1 IP complex but not in the IgY and IgG control (Fig. 2*E*, *lanes 1*, *4*, and *5*). However, the level of Ku70 and CANX in the IP complex (comparing *lanes 1* and *2*) was extremely low compared with the supernatant, suggesting that there are free forms of Ku70 and CANX. We were not able to detect NDRG1 in the IP complexes when the IP was

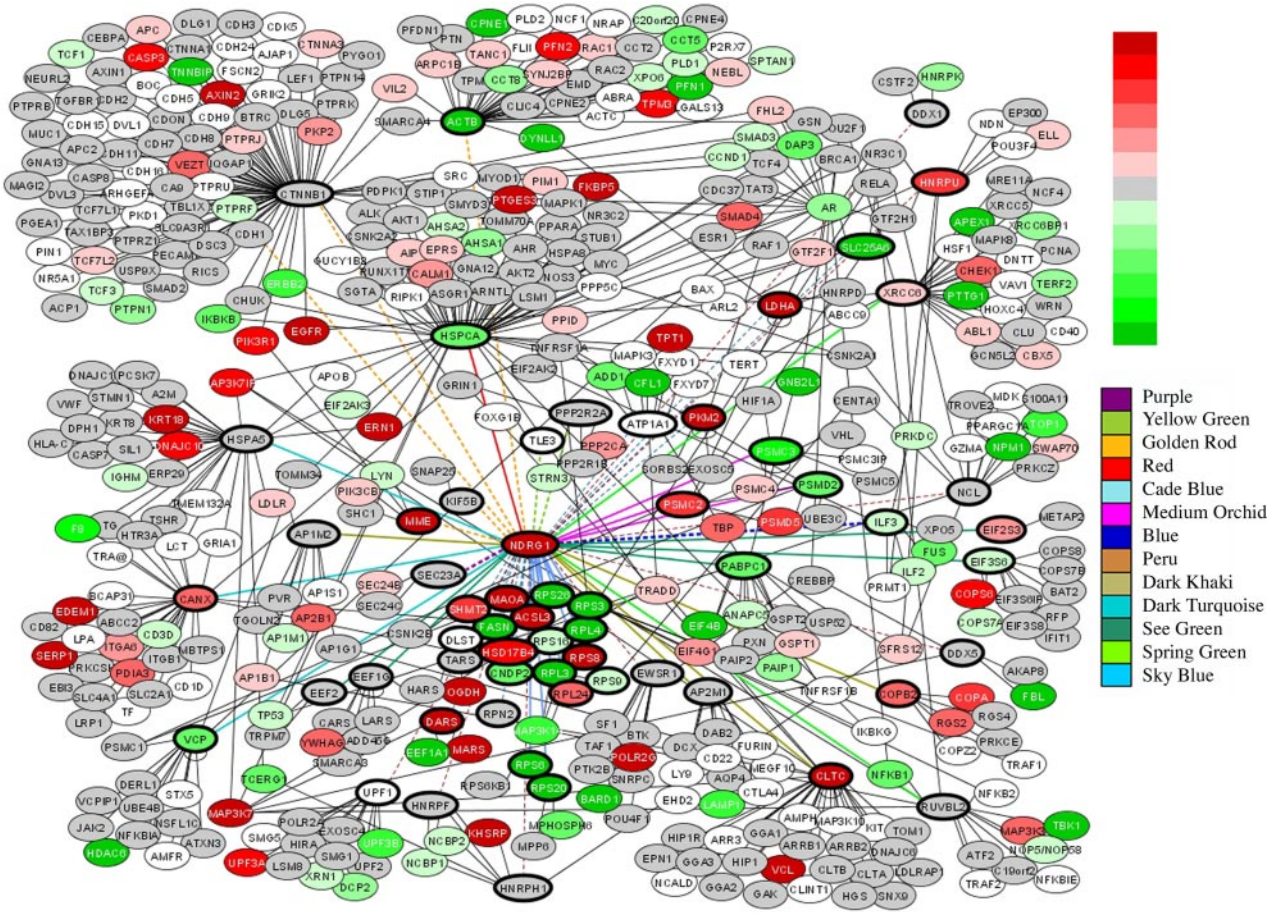

FIG. 1. **The NDRG1 interactome map.** The diagram shows all proteins (nodes) that appear at least three times in three independent IP/MS/MS experiments and their interactions (edges) that were retrieved from the HPRD (www.hprd.org). We retrieved only the first layer of the protein-protein interaction from the HPRD. To simplify the displayed map, we excluded from this figure many known interacting proteins of AR that do not show link to the NDRG1 interactome. The node color indicates mRNA expression level in response to androgen based on MPSS analysis of LNCaP cells treated with R1881 *versus* untreated cells. *Red*, androgen up-regulated (p value < 0.05); *green*, androgen down-regulated ($p < 0.05$); *gray*, no significant differences; *white*, not found in MPSS. The *color shade* from *bright* to *light* indicates high to low expression levels. The nodes with *thick borders* indicate NDRG1 interactors from our study (Table I), whereas the nodes with *thin borders* indicate interacting proteins derived from the HPRD. The *colored edges* represent different functional categories of proteins. *Solid lines*: *sky blue*, ribosomal proteins; *spring green*, DNA repair proteins; *sea green*, protein translation regulators; *dark turquoise*, ER resident chaperon proteins; *dark khaki*, intracellular trafficking of receptors and endocytosis; *medium orchid*, ubiquitin-dependent protein catabolism; *red*, chaperon protein. *Dashed lines*: *peru*, RNA processing; *purple*, ER to Golgi vesicle-mediated transport; *medium blue*, transcriptional factor; *cade blue*, metabolic enzymes, mitochondria precursors and carrier; *goldenrod*, cell adhesion and cytoskeleton organization; *yellow-green*, signal transduction. For those proteins for which no functional categories were shown, the color of the *edges* is *black*.

performed using anti-Ku70 or anti-CANX antibodies. However, this is likely because of the fact that most of the proteins pulled down by these two antibodies are the free forms, and only a small portion of these proteins were actually bound to NDRG1. The amount of bounded forms (to NDRG1) pulled down by anti-Ku70 or anti-CANX antibodies was too low to give a signal above background.

Non-genomic Function of the Interactome of NDRG1: NDRG1 Is Phosphorylated in LNCaP Cells, and the Phosphorylation Is Mediated by PKA—As shown in Fig. 2*A*, NDRG1 was phosphorylated in LNCaP cells (*upper band*, phosphorylated form), and the phosphorylation was dramatically increased after R1881 treatment.

To identify the phosphorylation site, we performed a SEQUEST database search with serine, threonine, and tyrosine phosphorylation as optional search parameters. We were able to identify three hits for the serine phosphorylated peptide R.TAS$_{167}$GSSVTSLDGTR.S with Peptide Prophet scores >0.95 (the dot in the peptide sequence indicates trpysin cleavage sites) and a single peptide hit for the threonine phosphorylated peptide R.SHT$_{181}$SEGAHLDITPNSGAAGNSAGPK.S. with a Peptide Prophet score of 0.97. Fig. 3 showed both the singly (y^+) and doubly charged (y^{2+}) y-ions of the phosphorylated (*bottom panel*) and unphosphorylated (*upper panel*) tryptic peptide R.TASGSSVTSLDGTR.S. We observed y12 ions for both the unphosphorylated form (*m/z* of

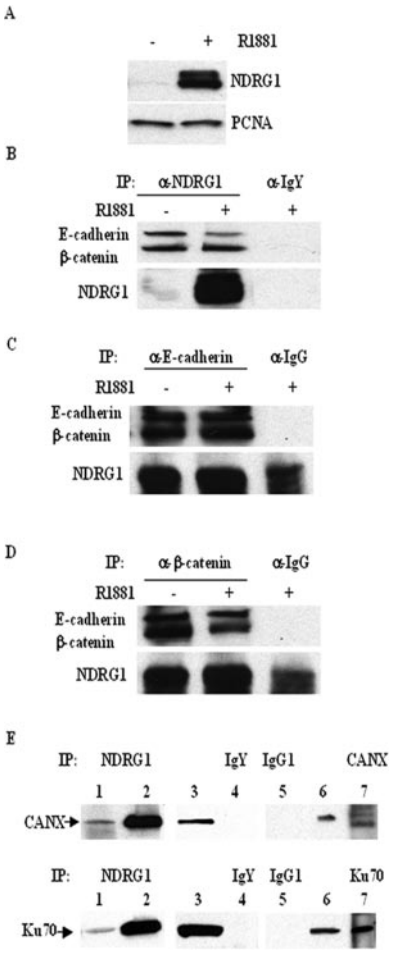

FIG. 2. **Western blot confirmation of the NDRG1 interactome.** *A*, Western blot showing that the expression of NDRG1 is induced dramatically by androgen. LNCaP cells were treated with 10 nM R1881 for 24 h. Cell lysates were collected and analyzed by SDS-PAGE and Western blotting. Blots were probed with antibodies against NDRG1 and PCNA. *B–D*, Western blot analyses of NDRG1 IP complex. LNCaP cells were treated with or without 10 nM R1881 for 24 h. Cell lysates were collected for coimmunoprecipitation using antibodies against *B*, NDRG1; *C*, E-cadherin; *D*, β-catenin; *E*, Ku70 and calnexin. IP complexes were separated by SDS-PAGE and analyzed by Western blotting. Blots were probed with antibodies against NDRG1, E-cadherin, β-catenin, Ku70, and calnexin. *E*, *lanes 1*, *4*, *5*, and *7* represent proteins from IP complexes. *lane 1*, anti-NDRG1; *lane 4*, anti-IgY; *lane 5*, anti-IgG1; *lane 7*, anti-CANX or anti-Ku70. *lanes 2*, *3*, and *6* represent proteins from the supernatant.

1167.2181, *upper panel*) and the phosphorylated form (*m/z* of 1247.2181, *bottom panel*) of the peptide. We also observed the doubly charged y12 ions for both phosphorylated and unphosphorylated forms (*m/z* 584.1130 and 624.1130, spectra not shown). The phosphorylated serine in the peptide $TAS_{167}GSSVTSLDGTR$ corresponds to the amino acid residue 330, and the phosphorylated threonine in the peptide $SHT_{181}SEGAHLDITPNSGAAGNSAGPK$ corresponds to the amino acid residue 366 of the NDRG1 protein sequence (RefSeq ID: NP_006087). Our data suggested that both phosphorylated and unphosphorylated forms of NDRG1 co-exist in cells. Other peptides with no phosphorylation sites were also identified and listed in Table II. We identified seven peptides with Peptide Prophet scores greater than 0.9. The total residues covered by these seven peptides are 82. However, among many putative phosphorylated amino acid residues in these 82 amino acid residues, only the two sites (serine 330 and threonine 366) were phosphorylated under our assessment conditions.

We utilized several kinase inhibitors to study which kinase mediates the phosphorylation of NDRG1 in LNCaP cells. LNCaP cells were pretreated with kinase inhibitors including the calmodulin kinase inhibitor KN-62, the cascein kinase II inhibitor DRB, the PKA inhibitor H89, and the PKC kinase inhibitor GF109230F for 30 min and then incubated with 10 nM R1881 for 24 h. Subsequently, cell lysates were prepared and analyzed for NDRG1 phosphorylation by Western blotting. As shown in Fig. 4, the phosphorylation of NDRG1 is reduced by all inhibitors that we tested. However, complete loss of phosphorylation was only observed in H89 (a PKA inhibitor)-treated cell lysates, suggesting that the phosphorylation of NDRG1 is prominently mediated by PKA. Our results were similar to the observation of Sugiki *et al.* (38) that NDRG1 undergoes phosphorylation in mast cells and that the phosphorylation depended on calmodulin kinase-II and PKA but not PKC. Interestingly, we also identified PPP2R2A (serine/threonine protein phosphatase 2A) as an NDRG1 interacting protein (Table I). This protein could potentially remove the phosphate in the NDRG1 protein added by PKA.

Non-genomic Function of the Interactome of NDRG1: NDRG1 Is Implicated in the ER Stress Response and Proteasome Activity—NDRG1 was postulated to play a role in ER stress response (39), and some NDRG1 interacting proteins that we identified were also involved in the ER stress response (Table I). To investigate whether changes in NDRG1 protein levels alter the protein levels of ER stress response proteins, siRNA interference was applied to knock-down the level of NDRG1 in LNCaP cells followed by measurement of expression levels of two ER stress inducible chaperon proteins GRP78 (HSPA5, heat shock 70 kDa protein 5) and GRP94 (HSP90B1, heat shock protein 90kDa β, member 1).

LNCaP cells were transfected with siRNA against NDRG1 and treated with or without 10 nM R1881. Cell lysates were collected at 72 h after treatments, and two ER stress markers (GRP78 and GRP94) were analyzed by Western blotting. PCNA was used as a loading control because its expression is unaffected by either R1881 or NDRG1 siRNA. As shown in Fig. 5*A*, in the absence of R1881 the level of NDRG1 was dramatically reduced in siRNA-transfected cells as compared with mock-transfected cells, and the level of GRP94 but not GRP78 was decreased under the NDRG1 knock-down condition (*lane 2 versus lane 1*), suggesting that NDRG1 may modulate ER inducible gene expression. Despite the fact that the level of NDRG1 was decreased by siRNA, it remained

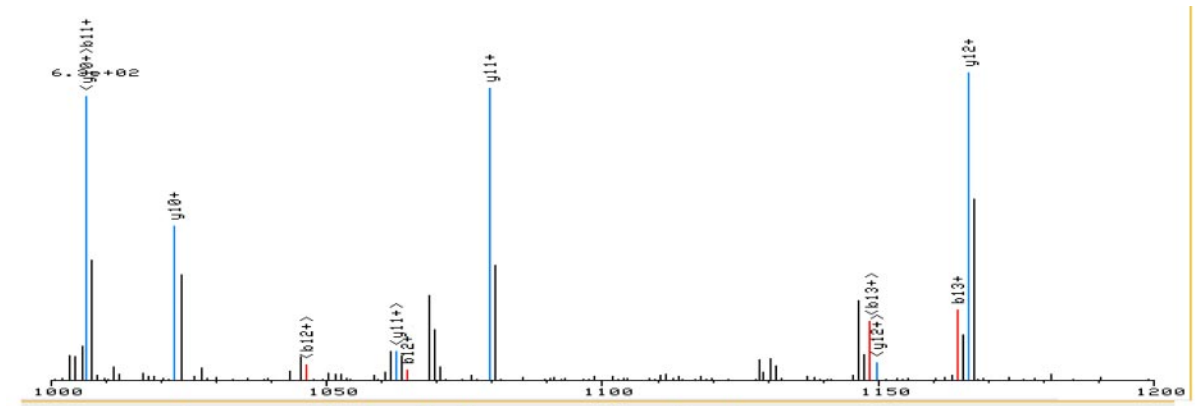

b+	#	AA	#	y+	y2+
102.1130	1	T	14		
173.1918	2	A	13	1238.2969	619.6524
260.2700	3	S	12	1167.2181	584.1130
317.3219	4	G	11	1080.1399	540.5739
404.4001	5	S	10	1023.0880	512.0480
491.4783	6	S	9	936.0098	468.5089
590.6109	7	V	8	848.9316	424.9698
691.7160	8	T	7	749.7990	375.4035
778.7942	9	S	6	648.6939	324.8509
891.9536	10	L	5	561.6157	281.3118
1007.0422	11	D	4	448.4563	224.7321
1064.0941	12	G	3	333.3677	167.1878
1165.1992	13	T	2	276.3158	138.6619
	14	R	1	175.2107	88.1093

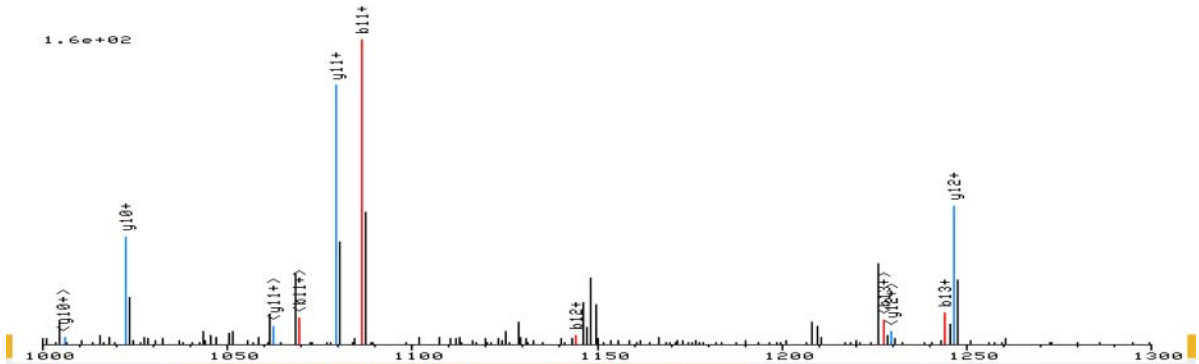

b+	#	AA	#	y+	y2+
102.1130	1	T	14		
173.1918	2	A	13	1318.2969	659.6524
340.2700	3	S	12	1247.2181	624.1130
397.3219	4	G	11	1080.1399	540.5739
484.4001	5	S	10	1023.0880	512.0480
571.4783	6	S	9	936.0098	468.5089
670.6109	7	V	8	848.9316	424.9698
771.7160	8	T	7	749.7990	375.4035
858.7942	9	S	6	648.6939	324.8509
971.9536	10	L	5	561.6157	281.3118
1087.0422	11	D	4	448.4563	224.7321
1144.0941	12	G	3	333.3677	167.1878
1245.1992	13	T	2	276.3158	138.6619
	14	R	1	175.2107	88.1093

S(3):+167.08

FIG. 3. **Close up view of the spectra of the phosphorylated and unphosphorylated peptide TASGSSVTSLDGTR of NDRG1.** Only the zoomed spectra in the *m/z* range between 1000 and 1200 were shown to show the singly charged y12+ ions clearly. Both the singly (y^{+}) and doubly charged (y^{2+}) y-ions of the phosphorylated (*bottom panel*) and unphosphorylated (*upper panel*) tryptic peptide R.TASGSSVTSLDGTR.S were identified. The y12 ions for both the unphosphorylated form (*m/z* 1167.2181, *upper panel*) and the phosphorylated form (*m/z* 1247.2181, *bottom panel*) of the peptide are shown. The spectra for the doubly charged y12 ions for both phosphorylated and unphosphorylated forms (*m/z* 584.1130 and 624.1130) are not shown; only the identification was indicated in the *table below* the close up view of the spectra *panels*.

TABLE II
NDRG1 peptides identified from our MS/MS analysis
The dots in the peptide sequences indicate trypsin cleavage sites.

Peptide sequences	No. of peptide hits	Peptide Prophet scores
R.SHTSEGAHLDITPNSGAAGNSAGPK.S	1	1
K.MADCGGLPQISQPAK.L	5	0.9979–9999
K.SIIGMGTGAGAY.I	2	0.9861–0.9886
R.EMQDVDLAEVKPLVEK.G	3	0.9538–1
R.SHT181SEGAHLDITPNSGAAGNSAGPK.S	1	0.9694
R.TAS167GSSVTSLDGTR.S	3	0.9477–0.9694
R.TASGSSVTSLDGTR.S	4	0.9996–1

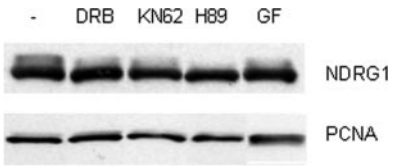

FIG. 4. **PKA mediates NDRG1 phosphorylation.** LNCaP cells were pretreated with serine/threonine kinase inhibitors as indicated for 30 min prior to treatment with 10 nM R1881 for 24 h. Cell lysates were prepared and proteins were separated by SDS-PAGE and immunoblotted with anti-NDRG1 and anti-PCNA. *GF*, chemical GF109203X from Sigma.

inducible in the presence of R1881 (*lane 4 versus lane 2*). The level of GRP94 was also inducible by R1881 (*lanes 3* and *4 versus lanes 1* and *2*). Unlike GRP94, the level of GRP78 was not altered regardless of the level of NDRG1.

ER stress response can activate ER-associated protein degradation, which is executed by proteasomes in the cytosol to relieve the overwhelmed stress in the ER (40). Because many of the proteasome subunits were identified in NDRG1 complex (Table I), it would be interesting to investigate whether NDRG1 plays a role in the regulation of proteasome activity. The proteasome possesses multiple peptidase activities including chymotrypsin-like activity, postglutamyl peptidase activity, and trypsin-like activity (41). We utilized a fluorogenic peptide substrate to measure the chymotrypsin-like activity of the proteasome under the NDRG1 suppressed condition. LNCaP cells were transfected with siRNA against NDRG1 and treated with or without 10 nM R1881. Cell lysates were collected 72 h after treatments, and the proteasome activity was measured using fluorogenic assays. As shown in Fig. 5*B* (*left panel*), in the absence of R1881, the proteasome activity was increased 45.5 ± 8% in NDRG1 siRNA transfected cells (*column b*) compared with mock-transfected cells (*column a*). R1881 itself increased proteasome activity (32.56 ± 16.46%) in the mock (non-NDRG1 knock-down) condition (comparing *column c* to *a*). Intriguingly, in the presence of R1881, knock-down of NDRG1 did not significantly alter R1881-enhanced proteasome activity (comparing *column c* to *d*). Under the NDRG1 knock-down condition, we observed no significant differences regardless of the presence or absence of R1881 (comparing *column d* to *b*). These

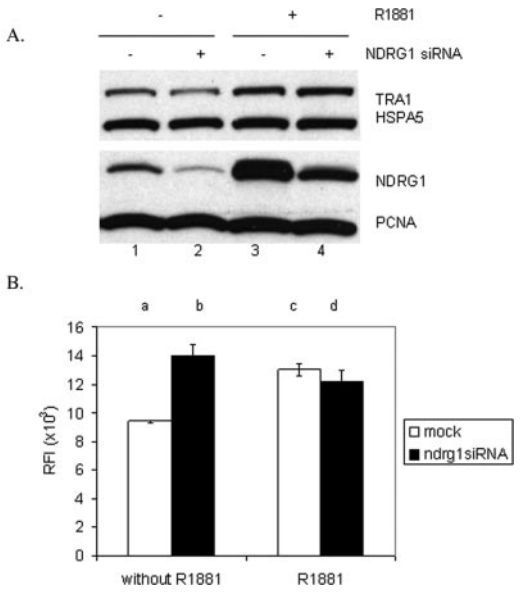

FIG. 5. **Measurement of the effects of NDRG1 on ER stress responses and proteasome activity.** LNCaP cells were transfected with an siRNA against NDRG1 and were treated with or without 10 nM R1881. Cell lysates were collected 72 h after incubation. *A*, proteins were subjected to SDS-PAGE and immunoblotted with anit-NDRG1, anti-KDEL (which recognizes both GRP78 and -94), and PCNA. *B*, cell lysates were subjected to proteasome activity assays by incubating with a fluorogenic substrate Suc-LLVY-AMC for 30 min. Release of the fluorescent group 7-amido-4-methylcoumarin from the proteasome substrate Suc-LLVY-AMC was monitored in a fluorescence plate (excitation/emission, 380/460 nm). The proteasome activities were represented as the fluorescence intensity ($n = 3$).

results suggested that NDRG1 plays a negative regulatory role on proteasome activity.

DISCUSSION

The role(s) of NDRG1 in tumor progression, invasion, and metastasis remains somewhat enigmatic and controversial. To understand the protein network by which NDRG1 executes its biological functions, we performed a comprehensive analysis of the interactome of NDRG1 in the androgen responsive LNCaP cell line using co-IP and tandem MS (Table I). We adopted a very stringent criterion to filter out those proteins that were not identified in three independent biological repli-

cates as well as those proteins that were seen in the control IP experiment; even so some abundant proteins may still be carried forward. We identified ribosomal proteins in our list (Table I). These ribosomal proteins may be contaminants in our IP experiment because of their abundance. Alternatively, some membrane-bound ribosomal proteins may co-IP with ER stress response proteins and thus be identified in our MS/MS data. For example, an ER transmembrane chaperon CANX was shown to interact directly with membrane-bound ribosome proteins including RPL4 and RPS9 (42, 43).

We identified 58 novel NDRG1 interacting proteins by IP-LC/MS/MS and tried to confirm their interaction using reciprocal co-IP. Among 58 proteins, only 16 of them have antibody available. We have tried all 16 antibodies. We were able to confirm the interaction of β-catenin, E-cadherin, and NDRG1 using reciprocal IP experiments. Initially we were perplexed because we were able to detect Ku70 and CANX when the IP was performed by the anti-NDRG1 antibody and the Western blot was performed using the anti-Ku70 or the anti-CANX antibodies, but we were not able to detect NDRG1 when the IP experiments were performed using the anti-Ku70 or the anti-CANX antibodies and Western blot was performed using the anti-NDRG1 antibody (Fig. 2). Additional experiments suggested that cells contain significant amount of NDRG1-bound β-catenin and E-cadherin. However, the level of NDRG1-bound Ku70 and CANX is extremely low compared with the level of Ku70 and CANX in total cell lysates, suggesting that most of the Ku70 and CANX exist as free forms or the interactions are transient, *i.e.* only exist when they are needed. When the amount of NDRG1-bound Ku70 and CANX proteins are much lower than that of the unbound forms, it is not surprising that an IP experiment can be directional, *i.e.* depending on which antibody is used in the IP and which is used in the Western blot analysis after IP. Alternatively, difference in the quality of antibodies for IP experiments can also play a role. As shown in Fig. 2*E* (*top panel*, *lane 7*), CANX antibody did not work well in IP. Many other factors can contribute to the success of an co-IP experiment including 1) the quality and efficiency of antibody to pull down the target protein, 2) the level of the bounded form to free forms for a specific interacting protein, 3) whether the epitope of an antibody is also involved in protein interaction and therefore is mutually exclusive (*i.e.* if bound to antibody, it may prevent it from binding to the interacting protein), 4) whether the protein-protein interaction is direct or indirect, lasting or transient etc. In addition, reciprocal IP experiments are tedious and not amenable for high throughput analysis. Therefore, alternative strategies such as fluorescence resonance energy transfer may be needed to confirm interacting proteins identified by large scale proteomics studies.

As part of our proteomics analysis, we also determined that two positions, serine residue 330 and threonine residue 366 of the NDRG1 protein (RefSeq ID: NP_006087) were phosphorylated under our assessment conditions, whereas the other putative residues among the 82 total amino acid residues we found in MS/MS analysis were not phosphorylated (Table II). Integration of our IP/MS/MS data with HPRD data suggested that NDRG1 forms a complex with β-catenin and androgen receptor, two key control proteins in cells (Fig. 2). It is well known that androgen mediates its action by binding to an androgen receptor. Upon androgen binding, the androgen receptor translocates from the cytosol to the nucleus and transactivates downstream genes (44). To respond to androgen quickly, the androgen receptor recruits different co-regulators such as heat shock proteins (Hsp), co-chaperones, and tetratricopeptide repeat containing proteins to obtain appropriate conformation changes upon androgen binding (45). Although we did not identify the androgen receptor itself in the NDRG1 complex, we identified three androgen receptor co-regulators: HSPCA, CTNNB1, and XRCC6 protein. HSPCA is known to bind to AR when it is in a ligand-unbound state (46). The HSPCA-AR complex then binds androgen (46). The binding is important for the stability and activation of AR as it has been demonstrated that AR is transformed into a DNA binding competent status with the assistance of HSPCA; AR then initiates nuclear translocation, recruitment of cofactors, and transactivation of target genes (47). CTNNB1 is a co-activator of the androgen receptor and a component of the Wnt signaling pathway (48). CTNNB1can promote androgen signaling by binding to the liganded AR, which leads to the transactivation of androgen-regulated genes (49, 50). XRCC6 and Ku80 were recently demonstrated to bind to AR and act as co-activator of AR (51). Ku80 was excluded from the 58 interacting proteins (Table I) because it was only identified in two of three replicate experiments.

We also overlaid the expression changes in response to androgen for the proteins in the NDRG1 interactome (Fig. 1). The intergrated interactome map provides an overview of a dynamic (dual) mode of the NDRG1 interactome. It is a first step toward a better understanding of the interactions between the androgen response program and the NDRG1 interactome as well as the effects and roles of these interactions in prostate cancer progression.

We showed that cell adhesion molecules including E-cadherin and β-catenin interact with NDRG1. The interaction of NDRG1 with E-cadherin or β-catenin is not affected by androgen stimulation (Fig. 2, *B–D*) or by the phosphorylation status of NDRG1 (data not shown). E-cadherin, β-catenin, and α-catenin are known to form a network in the adhesion junction (52). E-cadherin is a transmembrane protein having an extracellular domain that mediates homotypic cell-to-cell adhesion and a cytoplasmic tail that links to β-catenin and α-catenin, which in turn provides anchorage to the actin cytoskeleton. The loss of E-cadherin or disruption of cadherin-catenin interaction is known to increase the potential of metastasis in various tumors including prostate cancer (37). It was postulated that NDRG1 is functionally linked to the formation of the E-cadherin-β-catenin complex (53). Our study provides di-

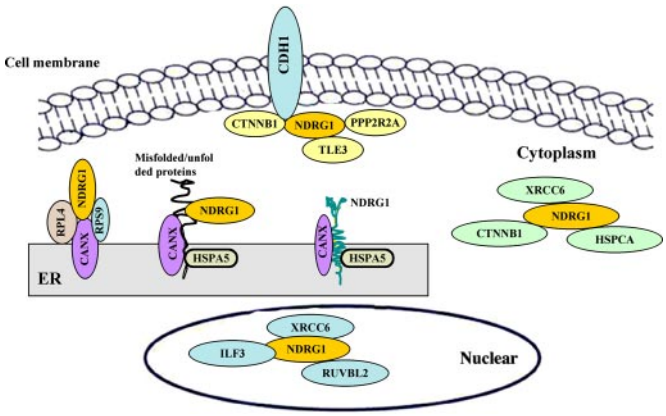

FIG. 6. **Our proposed model of the NDRG1 interactome indicating several modules of NDRG1 interactome.** In the cytosol, NDRG1 can form complex with TLE3 and PPP2R2A, two protein kinases. NDRG1 can form complex with ER chaperons, suggesting that either NDRG1 is a target to be folded into correct conformation by chaperons or acts as a chaperon itself. The complex of NDRG1 and AR co-regulators including CTNNB1, HSPCA, and XRCC6 could be in the cytosol or in the nuclear because these AR co-regulators can be distributed to both compartments.

rect evidence that NDRG1 forms a complex with both E-cadherin and β-catenin, probably close to the cellular junction.

We also identified ER stress response proteins in the NDRG1 complex including HSPA5, CANX, and transitional endoplasmic reticulum ATPase (VCP) in NDRG1 complex (Table I). NDRG1 is a known component of the ER stress response because it is sensitive to the redox status of the cells and the intracellular calcium concentration (16, 39). We showed that the expression of HSPA5 was not affected by NDRG1 knock-down, but the ER inducible chaperon protein TRA1 was decreased after knocking down NDRG1 in LNCaP cells (Fig. 5*A*), indicating that NDRG1 is involved in the induction of ER inducible chaperons. CANX is another chaperone that is structurally different from molecular chaperones of the Hsp60, Hsp70, and Hsp90 families (54) and is involved in the retention of incorrectly or incompletely folded proteins (54). VCP, the 97-kDa valosin containing protein is another chaperone that was shown to be associated with Hsp90 (55). We showed that NDRG1 interacted with these three chaperones, suggesting that NDRG1 might be a chaperon protein itself or the target of these chaperons (Fig. 6). Further experimentation is necessary to sort this out.

The proteasome is an essential component of the ATP-dependent proteolytic pathway that is responsible for the degradation of most cellular proteins (41). 26S proteosome is a multimeric protein complex that is composed of a 20S core particle and a 19S regulatory particle (41, 56). The 20S core particle possesses the catalytic activities that hydrolyze proteins into small pieces, whereas the 19S complex controls the entry of a substrate into the 20S core particle (41, 56). We identified several 19S subunits from the NDRG1 complex. We further showed that knocking down NDRG1 under androgen-starved conditions (no R1881) increases proteasomal activity (Fig. 5*B*). Androgen stimulation itself also increased proteasomal activity in native LNCaP cells that were not subject to NDRG1 knock-down (Fig 5*B*, *columns a* and *c*). However, the combination of androgen stimulation and NRDG1 knock-down (Fig 5*B*, *column d*) did not further increase proteasome activity (*i.e.* no additive effects). It is possible that androgen induction of NDRG1 expression counteracted the effect of NDRG1 knock-down and therefore could not have additive effects in increasing proteasome activity.

Proteasome activity is critical for androgen receptor transcriptional activity, as it was demonstrated that the inhibition of proteasome function attenuated androgen-induced AR nuclear translocation, whereas overexpression of PSMA7, a catalytic subunit of the 20S core particle, enhanced AR transactivation (57). We showed that androgen up-regulated PSMA7 but down-regulated several 19S subunits and proteasomal activators (Fig. 1). Our interactome map provides physical basis for the interaction between proteasome activity and the AR.

NDRG1 is localized in the cytoplasm (11). However, in response to p53 and DNA damage, NDRG1 can redistribute to the nucleus (58). The role of NDRG1 in the nucleus is unknown. We identified a transcriptional factor NFAT90 (ILF3) in the NDRG1 complex. This transcriptional factor in turn interacts with other transcriptional factors such as TP53, ILF2, FUS (fusion in t (12, 16) in malignant liposarcoma) (Fig. 1). These data suggest that NDRG1 may modulate the expression of genes that are controlled by these transcriptional factors.

We also identified several nucleoproteins such as XRCC6 and RuvB like-2 (RUVBL2) in the NDRG1 complex. XRCC6 is a regulatory subunit of a nuclear serine/threonine kinase DNA-dependent protein kinase that is involved in non-homologous end joining recombination (59, 60). RUVBL2 participates in DNA repair by driving the branch migration of the Holliday junction (61). DNA damage agents such as camptothecin can induce NDRG1 expression, and the induction seems to be associated with drug resistance (62). Our data suggest that the drug resistance may be caused by increased DNA repair ability induced by NDRG1 and its interactome.

Furthermore, some of the NDRG1 interacting proteins are also involved in the regulation of cell differentiation and tumor progression. Transducin-like enhancer protein 3 (TLE3) is a member of the Notch signaling pathway (63). This pathway controls the prostate epithelial cell differentiation and also is involved in prostate cancer progression. 17β-Hydroxysteroid dehydrogenase 4 (HSD17B4) catalyzes branched chain fatty acid β-oxidation in the peroxisome and works in the downstream from α-methylacyl-CoA racemase (AMACR). Both enzymes have been found to be up-regulated in human prostate cancer, and the selective up-regulation of peroxisomal branched chain fatty acid β-oxidation may be involved in the progression of prostate cancer (64). Further investigation of the interaction between NDRG1 and these proteins

may uncover the mechanisms by which NDRG1 induces differentiation.

Protein-protein interactions play critical roles in the biologic function of proteins. A proteome-wide approach such as IP/MS/MS was heralded as the method of choice for building a global protein interactome map (65). However, the limitation of the IP/MS/MS approach is that it cannot distinguish between direct and indirect interacting partners of a protein because both can be immunoprecipitated and therefore identified. The interacting proteins of NDRG1 we identified will contain both direct and indirect interacting proteins, and further experimentation is necessary to distinguish them. Furthermore, because NDRG1 is a protein with multiple possible cellular localizations (10, 66) and we only performed IP from the total cell lysates (not from different cellular compartments), our interactome map will be a combination of interactomes of all possible combinations. Nonetheless, we were able to identify different interactome modules at different cellular localization by the specific localization of the NDRG1 interacting proteins. For example, NDRG1-E-cadherin-β-catenin complex is likely to form at cellular junctions because E-cadherin is a cellular membrane transmembrane protein. The NDRG1-ILF3-XRCC6 complex is likely to form in the nucleus because ILF3 and XRCC6 are DNA binding proteins. We propose a model in which NDRG1 is associated with its interacting proteins at different cellular compartments as shown in Fig. 6. As we discussed earlier, NDRG1 is associated with chaperon proteins HSPA5, CANX, and VCP in ER. While in the cytosol, NDRG1 can bind to proteins like TLE3 and participate in signal transduction. The complex of NDRG1 and AR co-regulators including CTNNB1, HSPCA, and XRCC6 could be in the cytosol or in the nucleus because these AR co-regulators can be distributed to both compartments (67–69). The androgen receptor can promote CTNNB1 nuclear translocation (70). It is possible that NDRG1, which binds to CTNNB1, also plays a role in the AR-mediated transport of CTNNB1 to the nucleus. Multiple localization and interaction with multiple proteins may explain the multiple roles of NDRG1 in response to a variety of stimuli.

In summary, we have built a comprehensive interactome map of NDRG1, a versatile and a multiple functional molecule in the cell. This interactome map consists of several modules, which correspond to the reported functions of NDRG1. We also provide evidence suggesting that the NDRG1 interactome interacts closely with the androgen response program and that the expression of many genes in the interactome is affected by androgen. This interactome map provides the first road map for understanding the pleiotropic functions of NDRG1 at cellular level and its roles in human diseases.

Acknowledgments—We thank Dr. Jeff Ranish for the insightful discussions and Dr. David Goodlett, James White, and Joshua Tasman for critical reading of and comments on the manuscript.

* This publication was made possible by Grants 5P01CA085859, 5P50CA097186, 1P50GM076547, 1U54DA021519, and 1U54CA119347 from the National Institutes of Health (NIH), and its contents are solely the responsibility of the authors and do not necessarily represent the official views of the NIH. The costs of publication of this article were defrayed in part by the payment of page charges. This article must therefore be hereby marked "*advertisement*" in accordance with 18 U.S.C. Section 1734 solely to indicate this fact.

[S] The on-line version of this article (available at http://www.mcponline.org) contains supplemental Doc 1.

‡ To whom correspondence should be addressed: The Institute for Systems Biology, 1441 N. 34th Street, Seattle, WA 98103. Tel.: 206-732-1297; Fax: 206-732-1299; E-mail: blin@systemsbiology.org.

REFERENCES

1. Okuda, T., Kokame, K., and Miyata, T. (2005) Functional analyses of NDRG1, a stress-responsive gene. *Seikagaku* **77,** 630–634
2. Chen, B., Nelson, D. M., and Sadovsky, Y. (2006) N-myc down-regulated gene 1 modulates the response of term human trophoblasts to hypoxic injury. *J. Biol. Chem.* **281,** 2764–2772
3. Taketomi, Y., Sugiki, T., Saito, T., Ishii, S., Hisada, M., Suzuki-Nishimura, T., Uchida, M. K., Moon, T. C., Chang, H. W., Natori, Y., Miyazawa, S., Kikuchi-Yanoshita, R., Murakami, M., and Kudo, I. (2003) Identification of NDRG1 as an early inducible gene during in vitro maturation of cultured mast cells. *Biochem. Biophys. Res. Commun.* **306,** 339–346
4. Lachat, P., Shaw, P., Gebhard, S., van Belzen, N., Chaubert, P., and Bosman, F. T. (2002) Expression of NDRG1, a differentiation-related gene, in human tissues. *Histochem. Cell Biol.* **118,** 399–408
5. Li, J., and Kretzner, L. (2003) The growth-inhibitory Ndrg1 gene is a Myc negative target in human neuroblastomas and other cell types with overexpressed N- or c-myc. *Mol. Cell Biochem.* **250,** 91–105
6. Bandyopadhyay, S., Pai, S. K., Gross, S. C., Hirota, S., Hosobe, S., Miura, K., Saito, K., Commes, T., Hayashi, S., Watabe, M., and Watabe, K. (2003) The Drg-1 gene suppresses tumor metastasis in prostate cancer. *Cancer Res.* **63,** 1731–1736
7. Bandyopadhyay, S., Pai, S. K., Hirota, S., Hosobe, S., Tsukada, T., Miura, K., Takano, Y., Saito, K., Commes, T., Piquemal, D., Watabe, M., Gross, S., Wang, Y., Huggenvik, J., and Watabe, K. (2004) PTEN up-regulates the tumor metastasis suppressor gene Drg-1 in prostate and breast cancer. *Cancer Res.* **64,** 7655–7660
8. Guan, R. J., Ford, H. L., Fu, Y., Li, Y., Shaw, L. M., and Pardee, A. B. (2000) Drg-1 as a differentiation-related, putative metastatic suppressor gene in human colon cancer. *Cancer Res.* **60,** 749–755
9. Cangul, H., Salnikow, K., Yee, H., Zagzag, D., Commes, T., and Costa, M. (2002) Enhanced expression of a novel protein in human cancer cells: a potential aid to cancer diagnosis. *Cell Biol. Toxicol.* **18,** 87–96
10. Kurdistani, S. K., Arizti, P., Reimer, C. L., Sugrue, M. M., Aaronson, S. A., and Lee, S. W. (1998) Inhibition of tumor cell growth by RTP/rit42 and its responsiveness to p53 and DNA damage. *Cancer Res.* **58,** 4439–4444
11. van Belzen, N., Dinjens, W. N., Diesveld, M. P., Groen, N. A., van der Made, A. C., Nozawa, Y., Vlietstra, R., Trapman, J., and Bosman, F. T. (1997) A novel gene which is up-regulated during colon epithelial cell differentiation and down-regulated in colorectal neoplasms. *Lab. Invest.* **77,** 85–92
12. Wang, Z., Wang, F., Wang, W. Q., Gao, Q., Wei, W. L., Yang, Y., and Wang, G. Y. (2004) Correlation of N-myc downstream-regulated gene 1 overexpression with progressive growth of colorectal neoplasm. *World J. Gastroenterol.* **10,** 550–554
13. Zhou, R. H., Kokame, K., Tsukamoto, Y., Yutani, C., Kato, H., and Miyata, T. (2001) Characterization of the human NDRG gene family: a newly identified member, NDRG4, is specifically expressed in brain and heart. *Genomics* **73,** 86–97
14. Agarwala, K. L., Kokame, K., Kato, H., and Miyata, T. (2000) Phosphorylation of RTP, an ER stress-responsive cytoplasmic protein. *Biochem. Biophys. Res. Commun.* **272,** 641–647
15. Shaw, E., McCue, L. A., Lawrence, C. E., and Dordick, J. S. (2002) Identification of a novel class in the alpha/beta hydrolase fold superfamily: the N-myc differentiation-related proteins. *Proteins* **47,** 163–168
16. Kokame, K., Kato, H., and Miyata, T. (1996) Homocysteine-respondent genes in vascular endothelial cells identified by differential display anal-

ysis. GRP78/BiP and novel genes. *J. Biol. Chem.* **271,** 29659–29665
17. Lin, T. M., and Chang, C. (1997) Cloning and characterization of TDD5, an androgen target gene that is differentially repressed by testosterone and dihydrotestosterone. *Proc. Natl. Acad. Sci. U. S. A.* **94,** 4988–4993
18. Nelson, P. S., Clegg, N., Arnold, H., Ferguson, C., Bonham, M., White, J., Hood, L., and Lin, B. (2002) The program of androgen-responsive genes in neoplastic prostate epithelium. *Proc. Natl. Acad. Sci. U. S. A.* **99,** 11890–11895
19. Zhou, D., Salnikow, K., and Costa, M. (1998) Cap43, a novel gene specifically induced by Ni^{2+} compounds. *Cancer Res.* **58,** 2182–2189
20. Salnikow, K., Su, W., Blagosklonny, M. V., and Costa, M. (2000) Carcinogenic metals induce hypoxia-inducible factor-stimulated transcription by reactive oxygen species-independent mechanism. *Cancer Res.* **60,** 3375–3378
21. Salnikow, K., Li, X., and Lippmann, M. (2004) Effect of nickel and iron co-exposure on human lung cells. *Toxicol. Appl. Pharmacol.* **196,** 258–265
22. Wimmer, U., Wang, Y., Georgiev, O., and Schaffner, W. (2005) Two major branches of anti-cadmium defense in the mouse: MTF-1/metallothioneins and glutathione. *Nucleic Acids Res.* **33,** 5715–5727
23. Shah, M. A., Kemeny, N., Hummer, A., Drobnjak, M., Motwani, M., Cordon-Cardo, C., Gonen, M., and Schwartz, G. K. (2005) Drg1 expression in 131 colorectal liver metastases: correlation with clinical variables and patient outcomes. *Clin. Cancer Res.* **11,** 3296–3302
24. Salnikow, K., Kluz, T., and Costa, M. (1999) Role of $Ca^{(2+)}$ in the regulation of nickel-inducible Cap43 gene expression. *Toxicol. Appl. Pharmacol.* **160,** 127–132
25. Salnikow, K., Blagosklonny, M. V., Ryan, H., Johnson, R., and Costa, M. (2000) Carcinogenic nickel induces genes involved with hypoxic stress. *Cancer Res.* **60,** 38–41
26. Cangul, H., Salnikow, K., Yee, H., Zagzag, D., Commes, T., and Costa, M. (2002) Enhanced overexpression of an HIF-1/hypoxia-related protein in cancer cells. *Environ. Health Perspect.* **110 (Suppl 5),** 783–788
27. Semenza, G. L. (1998) Hypoxia-inducible factor 1: master regulator of O2 homeostasis. *Curr. Opin. Genet. Dev.* **8,** 588–594
28. Li, J., Davidson, G., Huang, Y., Jiang, B. H., Shi, X., Costa, M., and Huang, C. (2004) Nickel compounds act through phosphatidylinositol-3-kinase/Akt-dependent, p70(S6k)-independent pathway to induce hypoxia inducible factor transactivation and Cap43 expression in mouse epidermal Cl41 cells. *Cancer Res.* **64,** 94–101
29. Salnikow, K., Kluz, T., Costa, M., Piquemal, D., Demidenko, Z. N., Xie, K., and Blagosklonny, M. V. (2002) The regulation of hypoxic genes by calcium involves c-Jun/AP-1, which cooperates with hypoxia-inducible factor 1 in response to hypoxia. *Mol. Cell. Biol.* **22,** 1734–1741
30. Keller, A., Nesvizhskii, A. I., Kolker, E., and Aebersold, R. (2002) Empirical statistical model to estimate the accuracy of peptide identifications made by MS/MS and database search. *Anal. Chem.* **74,** 5383–5392
31. Nesvizhskii, A. I., Keller, A., Kolker, E., and Aebersold, R. (2003) A statistical model for identifying proteins by tandem mass spectrometry. *Anal. Chem.* **75,** 4646–4658
32. Li, X. J., Zhang, H., Ranish, J. A., and Aebersold, R. (2003) Automated statistical analysis of protein abundance ratios from data generated by stable-isotope dilution and tandem mass spectrometry. *Anal. Chem.* **75,** 6648–6657
33. Pajonk, F., van Ophoven, A., and McBride, W. H. (2005) Hyperthermia-induced proteasome inhibition and loss of androgen receptor expression in human prostate cancer cells. *Cancer Res.* **65,** 4836–4843
34. Sugiki, T., Taketomi, Y., Kikuchi-Yanoshita, R., Murakami, M., and Kudo, I. (2004) Association of N-myc downregulated gene 1 with heat-shock cognate protein 70 in mast cells. *Biol. Pharm. Bull.* **27,** 628–633
35. Lin, B., White, J. T., Lu, W., Xie, T., Utleg, A. G., Yan, X., Yi, E. C., Shannon, P., Khrebtukova, I., Lange, P. H., Goodlett, D. R., Zhou, D., Vasicek, T. J., and Hood, L. (2005) Evidence for the presence of disease-perturbed networks in prostate cancer cells by genomic and proteomic analyses: a systems approach to disease. *Cancer Res.* **65,** 3081–3091
36. Brenner, S., Johnson, M., Bridgham, J., Golda, G., Lloyd, D. H., Johnson, D., Luo, S., McCurdy, S., Foy, M., Ewan, M., Roth, R., George, D., Eletr, S., Albrecht, G., Vermaas, E., Williams, S. R., Moon, K., Burcham, T., Pallas, M., DuBridge, R. B., Kirchner, J., Fearon, K., Mao, J., and Corcoran, K. (2000) Gene expression analysis by massively parallel signature sequencing (MPSS) on microbead arrays. *Nat. Biotechnol.* **18,** 630–634
37. Bracke, M. E., Van Roy, F. M., and Mareel, M. M. (1996) The E-cadherin/catenin complex in invasion and metastasis. *Curr. Top. Microbiol. Immunol.* **213 (Pt 1),** 123–161
38. Sugiki, T., Murakami, M., Taketomi, Y., Kikuchi-Yanoshita, R., and Kudo, I. (2004) N-myc downregulated gene 1 is a phosphorylated protein in mast cells. *Biol. Pharm. Bull.* **27,** 624–627
39. Kokame, K., Kato, H., and Miyata, T. (1998) Nonradioactive differential display cloning of genes induced by homocysteine in vascular endothelial cells. *Methods* **16,** 434–443
40. Nishikawa, S., Brodsky, J. L., and Nakatsukasa, K. (2005) Roles of molecular chaperones in endoplasmic reticulum (ER) quality control and ER-associated degradation (ERAD). *J. Biochem.* (*Tokyo*) **137,** 551–555
41. Coux, O., Tanaka, K., and Goldberg, A. L. (1996) Structure and functions of the 20S and 26S proteasomes. *Annu. Rev. Biochem.* **65,** 801–847
42. Chevet, E., Wong, H. N., Gerber, D., Cochet, C., Fazel, A., Cameron, P. H., Gushue, J. N., Thomas, D. Y., and Bergeron, J. J. (1999) Phosphorylation by CK2 and MAPK enhances calnexin association with ribosomes. *EMBO J.* **18,** 3655–3666
43. Delom, F., and Chevet, E. (2006) *In vitro* mapping of calnexin interaction with ribosomes. *Biochem. Biophys. Res. Commun.* **341,** 39–44
44. Simental, J. A., Sar, M., Lane, M. V., French, F. S., and Wilson, E. M. (1991) Transcriptional activation and nuclear targeting signals of the human androgen receptor. *J. Biol. Chem.* **266,** 510–518
45. Pratt, W. B., and Toft, D. O. (1997) Steroid receptor interactions with heat shock protein and immunophilin chaperones. *Endocr. Rev.* **18,** 306–360
46. Prescott, J., and Coetzee, G. A. (2006) Molecular chaperones throughout the life cycle of the androgen receptor. *Cancer Lett.* **231,** 12–19
47. Georget, V., Terouanne, B., Nicolas, J. C., and Sultan, C. (2002) Mechanism of antiandrogen action: key role of hsp90 in conformational change and transcriptional activity of the androgen receptor. *Biochemistry* **41,** 11824–11831
48. Linja, M. J., Porkka, K. P., Kang, Z., Savinainen, K. J., Janne, O. A., Tammela, T. L., Vessella, R. L., Palvimo, J. J., and Visakorpi, T. (2004) Expression of androgen receptor coregulators in prostate cancer. *Clin. Cancer Res.* **10,** 1032–1040
49. Yang, X., Chen, M. W., Terry, S., Vacherot, F., Bemis, D. L., Capodice, J., Kitajewski, J., de la Taille, A., Benson, M. C., Guo, Y., and Buttyan, R. (2006) Complex regulation of human androgen receptor expression by Wnt signaling in prostate cancer cells. *Oncogene* **25,** 3436–3444
50. Terry, S., Yang, X., Chen, M. W., Vacherot, F., and Buttyan, R. (2006) Multifaceted interaction between the androgen and Wnt signaling pathways and the implication for prostate cancer. *J. Cell. Biochem.* **99,** 402–410
51. Mayeur, G. L., Kung, W. J., Martinez, A., Izumiya, C., Chen, D. J., and Kung, H. J. (2005) Ku is a novel transcriptional recycling coactivator of the androgen receptor in prostate cancer cells. *J. Biol. Chem.* **280,** 10827–10833
52. Goodsell, D. S. (2002) The molecular perspective: cadherin. *Stem. Cells* **20,** 583–584
53. Yoshizumi, T., Ohta, T., Ninomiya, I., Terada, I., Fushida, S., Fujimura, T., Nishimura, G., Shimizu, K., Yi, S., and Miwa, K. (2004) Thiazolidinedione, a peroxisome proliferator-activated receptor-gamma ligand, inhibits growth and metastasis of HT-29 human colon cancer cells through differentiation-promoting effects. *Int. J. Oncol.* **25,** 631–639
54. Bergeron, J. J., Brenner, M. B., Thomas, D. Y., and Williams, D. B. (1994) Calnexin: a membrane-bound chaperone of the endoplasmic reticulum. *Trends Biochem. Sci.* **19,** 124–128
55. Prince, T., Shao, J., Matts, R. L., and Hartson, S. D. (2005) Evidence for chaperone heterocomplexes containing both Hsp90 and VCP. *Biochem. Biophys. Res. Commun.* **331,** 1331–1337
56. Schmidt, M., Hanna, J., Elsasser, S., and Finley, D. (2005) Proteasome-associated proteins: regulation of a proteolytic machine. *Biol. Chem.* **386,** 725–737
57. Lin, H. K., Altuwaijri, S., Lin, W. J., Kan, P. Y., Collins, L. L., and Chang, C. (2002) Proteasome activity is required for androgen receptor transcriptional activity via regulation of androgen receptor nuclear translocation and interaction with coregulators in prostate cancer cells. *J. Biol. Chem.* **277,** 36570–36576
58. Stein, S., Thomas, E. K., Herzog, B., Westfall, M. D., Rocheleau, J. V., Jackson, R. S., II, Wang, M., and Liang, P. (2004) NDRG1 is necessary for p53-dependent apoptosis. *J. Biol. Chem.* **279,** 48930–48940

59. Dvir, A., Peterson, S. R., Knuth, M. W., Lu, H., and Dynan, W. S. (1992) Ku autoantigen is the regulatory component of a template-associated protein kinase that phosphorylates RNA polymerase II. *Proc. Natl. Acad. Sci. U. S. A.* **89,** 11920–11924
60. Lees-Miller, S. P., Chen, Y. R., and Anderson, C. W. (1990) Human cells contain a DNA-activated protein kinase that phosphorylates simian virus 40 T antigen, mouse p53, and the human Ku autoantigen. *Mol. Cell. Biol.* **10,** 6472–6481
61. Makino, Y., Kanemaki, M., Kurokawa, Y., Koji, T., and Tamura, T. (1999) A rat RuvB-like protein, TIP49a, is a germ cell-enriched novel DNA helicase. *J. Biol. Chem.* **274,** 15329–15335
62. Shah, M. A., Kortmansky, J., Motwani, M., Drobnjak, M., Gonen, M., Yi, S., Weyerbacher, A., Cordon-Cardo, C., Lefkowitz, R., Brenner, B., O'Reilly, E., Saltz, L., Tong, W., Kelsen, D. P., and Schwartz, G. K. (2005) A phase I clinical trial of the sequential combination of irinotecan followed by flavopiridol. *Clin. Cancer Res.* **11,** 3836–3845
63. Liu, Y., Dehni, G., Purcell, K. J., Sokolow, J., Carcangiu, M. L., Artavanis-Tsakonas, S., and Stifani, S. (1996) Epithelial expression and chromosomal location of human TLE genes: implications for notch signaling and neoplasia. *Genomics* **31,** 58–64
64. Zha, S., Ferdinandusse, S., Hicks, J. L., Denis, S., Dunn, T. A., Wanders, R. J., Luo, J., De Marzo, A. M., and Isaacs, W. B. (2005) Peroxisomal branched chain fatty acid beta-oxidation pathway is upregulated in prostate cancer. *Prostate* **63,** 316–323
65. Mann, M., Hendrickson, R. C., and Pandey, A. (2001) Analysis of proteins and proteomes by mass spectrometry. *Annu. Rev. Biochem.* **70,** 437–473
66. Kim, K. T., Ongusaha, P. P., Hong, Y. K., Kurdistani, S. K., Nakamura, M., Lu, K. P., and Lee, S. W. (2004) Function of Drg1/Rit42 in p53-dependent mitotic spindle checkpoint. *J. Biol. Chem.* **279,** 38597–38602
67. Sena, P., Saviano, M., Monni, S., Losi, L., Roncucci, L., Marzona, L., and Pol, A. D. (2005) Subcellular localization of beta-catenin and APC proteins in colorectal preneoplastic and neoplastic lesions. *Cancer Lett.* **241,** 203–212
68. Gasc, J. M., Renoir, J. M., Faber, L. E., Delahaye, F., and Baulieu, E. E. (1990) Nuclear localization of two steroid receptor-associated proteins, hsp90 and p59. *Exp. Cell Res.* **186,** 362–367
69. Koike, M., Shiomi, T., and Koike, A. (2001) Dimerization and nuclear localization of ku proteins. *J. Biol. Chem.* **276,** 11167–11173
70. Mulholland, D. J., Cheng, H., Reid, K., Rennie, P. S., and Nelson, C. C. (2002) The androgen receptor can promote beta-catenin nuclear translocation independently of adenomatous polyposis coli. *J. Biol. Chem.* **277,** 17933–17943